Role of entropy in magnetotail dynamics

J. Birn,[1] M. Hesse,[2] K. Schindler,[3] and S. Zaharia[1]

Received 22 December 2008; revised 6 February 2009; accepted 18 February 2009; published 18 April 2009.

[1] The role of entropy conservation and loss in magnetotail dynamics, particularly in relation to substorm phases, is discussed on the basis of MHD theory and simulations, using comparisons with particle-in-cell (PIC) simulations for validation. Entropy conservation appears to be a crucial element leading to the formation of thin embedded current sheets in the late substorm growth phase and the potential loss of equilibrium. Entropy conservation also governs the accessibility of final states of evolution and the amount of energy that may be released. Entropy loss (in the form of plasmoids) is essential in the earthward transport of flux tubes (bubbles, bursty bulk flows). Entropy loss also changes the tail stability properties and may render ballooning modes unstable and thus contribute to cross-tail variability. We illustrate these effects through results from theory and simulations.

Citation: Birn, J., M. Hesse, K. Schindler, and S. Zaharia (2009), Role of entropy in magnetotail dynamics, *J. Geophys. Res.*, *114*, A00D03, doi:10.1029/2008JA014015.

1. Introduction

[2] In a simplified view, magnetospheric evolution and dynamics may be separated into phases that apparently are well described by the constraints of the ideal magnetohydrodynamic (MHD) equations, interrupted by phases in which one or more of the basic assumptions of ideal MHD breaks down. A major assumption of ideal MHD that governs topology conservation is the so-called "frozen-in" field approximation, which is equivalent to the neglect of the electric field in the plasma rest frame,

$$\mathbf{E} + \mathbf{v} \times \mathbf{B} = 0 \tag{1}$$

Although (1) appears to be a good approximation most of the time and over most of the magnetosphere, particularly when the charged particle motion is dominated by $\mathbf{E} \times \mathbf{B}$ drift, its temporal and local breakdown by magnetic reconnection is a crucial element in the transport across the magnetopause and the release of magnetic energy in the magnetotail related to substorms. This requires a local violation of the ideal MHD constraint (1) associated with a dissipative electric field

$$\mathbf{E}' = \mathbf{E} + \mathbf{v} \times \mathbf{B} \neq 0 \tag{2}$$

Many of the investigations of magnetic reconnection therefore have focused on the mechanisms for the breakdown of (1) and the properties of the dissipative electric field $\mathbf{E}'$, resulting basically from electron inertia effects [*Vasyliūnas*, 1975; *Lyons and Pridmore-Brown*, 1990; *Pritchett*, 1994; *Hesse and Winske*, 1998; *Shay and Drake*, 1998].

[3] Significantly less attention has been paid to additional assumptions that enter the one-fluid MHD equations and that might play an equally important role. These consist of the assumption of isotropic plasma pressure p and the neglect of heat flux or, more specifically, the divergence of the heat flux tensor. Here heat flux represents the third-order moment of the particle distribution function, representing thermal energy transport or conduction in the plasma rest frame. The latter assumptions lead to the adiabatic, i.e., entropy conserving law, which may be written as

$$\frac{d}{dt}\frac{p}{\rho^\gamma} = 0 \tag{3}$$

where ρ is the plasma density and $d/dt \equiv \partial/\partial t + \mathbf{v} \cdot \nabla$ is the time derivative in a comoving frame. Here $\gamma = 5/3$ is the adiabatic constant, appropriate for an isotropic plasma distribution function (taken in the plasma rest frame).

[4] Frequently, rather than investigating (3), an integral quantity pV^γ is used [e.g., *Wolf et al.*, 2006], where V is the volume of a magnetic flux tube of unit flux, defined by

$$V = \int \frac{ds}{B} \tag{4}$$

and s is the arc length along a magnetic field line. The quantity pV^γ is an entropy measure appropriate for slowly evolving magnetic flux tubes governed by ideal MHD in quasi-equilibrium, when p is constant along a field line.

[5] In addition to the breakdown of ideal MHD by local dissipation, the entropy conservation (3) and its breakdown may also have important implications for the stability and evolution of the magnetotail. This is the topic of the present paper. We note here that, for comparisons with MHD simulations, our entropy investigation is done within the

[1]Los Alamos National Laboratory, Los Alamos, New Mexico, USA.
[2]NASA Goddard Space Flight Center, Greenbelt, Maryland, USA.
[3]Institut für Theoretische Physik, Ruhr-Universität, Bochum, Germany.

Copyright 2009 by the American Geophysical Union.
0148-0227/09/2008JA014015

single-fluid approximation, without regards for properties of particle distribution functions. In section 2 we start out with a more precise definition of integral conservation laws applied to magnetic flux tubes and the relation to entropy. This is followed in section 3 by validity tests based on comparisons between MHD and particle simulations, complemented by equilibrium results that incorporate entropy conservation. In section 4 we address the particular role of entropy conservation for the substorm growth phase based on results from quasi-static theory and MHD simulations. As discussed in section 5, the subsequent loss of entropy by the severance of a plasmoid is relevant for transport and stability. The entropy loss not only enables depleted flux tubes to penetrate close to the Earth, but may also permit ballooning instabilities to provide cross-tail structure and filamentation.

2. Integral Conservation Laws

2.1. Basic Conserved Quantities

[6] We start out with a discussion of conserved quantities assuming, at first, the validity of ideal MHD. We use the frozen-flux theorem to identify moving flux tubes and assume that there are no losses or gains through the boundaries of the system. In that case the mass content of a flux tube of unit flux, defined by the integral along the field line,

$$M = \int \rho dV = \int \rho \frac{ds}{B} \tag{5}$$

is a conserved quantity, i.e., $dM/dt = 0$. Now let us assume that the magnetic field can be derived from Euler potentials α and β via

$$\mathbf{B} = \nabla\alpha \times \nabla\beta \tag{6}$$

Choosing a gauge in which α and β are constant within a frame moving with the plasma, $M(\alpha, \beta)$ is a conserved function. Using the conservation law (3), one can easily find that the quantity

$$S = \int p^{1/\gamma} \frac{ds}{B} = S(\alpha, \beta) \tag{7}$$

is also a conserved function.

[7] The quantity S is related to, but not identical with, the entropy of a flux tube of an ideal gas. The specific entropy of an ideal gas, i.e., the entropy per unit mass is given by

$$\sigma = R \ln\left(Cp^{1/\gamma}/\rho\right) \tag{8}$$

where R and C are constants. Then we can find the entropy Σ of a flux tube of unit magnetic flux by

$$\Sigma = \int \sigma\rho \frac{ds}{B} \tag{9}$$

We note that Σ, as well as the integral over any arbitrary function of σ, are also conserved quantities in ideal MHD.

[8] If σ is initially constant along field lines, then the frozen-in condition, together with the adiabatic law (3), ensure that it remains constant along evolving field lines, and we obtain $\Sigma = \sigma M$. Then we find from (7) and (8)

$$S = \frac{M}{C} \exp(\sigma/R) = \frac{M}{C} \exp(\Sigma/MR) \tag{10}$$

that is, S is a direct function of the entropy Σ (for given mass M).

[9] If both, p and ρ (and hence σ) are constant along field lines we find $M = \rho V$, and the quantity S in (7) becomes identical to

$$S = p^{1/\gamma} V \tag{11}$$

equivalent to pV^{γ} used by *Wolf et al.* [2006]. Obviously, the definition (11) is applicable only in relatively slowly evolving fields, governed by instantaneous equilibrium, or at the beginning and the end of a sequence that leads from one equilibrium to another. However, the quantities S and Σ, defined by equations (7) and (9), respectively, remain well defined and are conserved in ideal MHD, even if the pressure does not stay constant along field lines.

[10] Now let us assume that initially the specific entropy is not constant along field lines (for instance, as a result of reconnection between different plasma populations; see section 2.4) but that the system eventually relaxes into a new equilibrium with constant temperature, density, and entropy density along field lines, while maintaining pressure balance. Such a relaxation typically involves heat flux along field lines, not included in standard ideal MHD, and an increase in entropy Σ, defined by (9). However, the quantity S defined by (7) remains conserved if the relaxation does not involve dissipation and heat loss or gain through the boundaries of the system or across the magnetic field. In that case S is a measure of the entropy of the relaxed state rather than of the instantaneous entropy. This makes it more useful than the actual entropy for a comparison between particle simulations, which may include such a relaxation, and MHD, which usually does not. We note further that the evaluation of S given by equation (7), rather than any other function of σ, is also advantageous, because it does not require the knowledge of density and it can be used even in nonequilibrium. In the following we will denote S as given by (7) as "entropy function," but emphasize again that S may correspond to an upper bound of the entropy (disregarding entropy enhancement from dissipation), rather than the actual entropy.

2.2. Anisotropy

[11] Our investigations of entropy conservation include comparisons between MHD and particle-in-cell (PIC) simulations (see section 3). The pressure in the PIC simulations need not remain isotropic. However, if we postulate a pitch angle scattering process that isotropizes the pressure (while conserving energy), which is implied in MHD, then one can compare the MHD results with a pressure $\overline{p}$ defined by 1/3 of the trace of the full pressure tensor given by

$$\overline{p} = \frac{1}{3} \sum_{j=1}^{3} P_{jj} \tag{12}$$

using the sum of ion and electron pressure. If the pressure is gyrotropic, this can be written as

$$\overline{p} = \frac{1}{3}p_{\parallel} + \frac{2}{3}p_{\perp} \tag{13}$$

Alternatively one might consider double-adiabatic theory, which is based on the assumption of gyrotropy and the neglect of heat flux [*Chew et al.*, 1956]. In that case equation (3) can be applied when p is replaced by

$$\overline{p} = p_{\parallel}^{1/3} p_{\perp}^{2/3} \tag{14}$$

For modest deviations from isotropy the expressions (13) and (14) give very similar results. In fact in our calculation of the quantity S for the PIC simulation discussed in section 3 we have found no visible difference between using (13) and (14).

2.3. Systems With Invariance Along *y*

[12] In a 2(+1/2)-dimensional system with $\partial/\partial y = 0$ the magnetic field can be derived from Euler potentials

$$\alpha = A(x,z,t) \qquad \beta = y + b(x,z,t) \tag{15}$$

such that

$$\mathbf{B} = \nabla A \times \hat{\mathbf{y}} + B_y \hat{\mathbf{y}} \qquad B_y = (\nabla A \times \nabla b) \cdot \hat{\mathbf{y}} \tag{16}$$

Here $\hat{\mathbf{y}}$ is the unit vector in the y direction and B_y represents the so-called "guide field" in the invariant direction. In that case one obtains the conserved mass $M = M(A)$ and entropy function $S = S(A)$ as functions of a single flux variable A (choosing again a gauge in which A is invariant in a comoving frame, i.e., $dA/dt = 0$). For finite B_y one can identify a further nontrivial quantity which is conserved if the footpoints of field lines at the boundaries do not move: the displacement between two footpoints in the invariant direction y

$$Y(A) = \int dy = \int B_y ds/B \tag{17}$$

In quasi-equilibrium, B_y is constant along field lines and thus (17) can be written as a conservation law similar to (11)

$$Y(A) = B_y V \tag{18}$$

The functions $V(A)$ and $B_y(A)$ typically change for an evolution that leads from one equilibrium to another one (or through a sequence of quasi-static equilibria). However, the function $Y(A)$ remains conserved if the field line footpoints remain fixed. We note that a 2.5-D equilibrium is governed by the Grad-Shafranov equation

$$-\nabla^2 A = \frac{d}{dA}\left(\mu_0 p + B_y^2/2\right) \tag{19}$$

Plasma pressure p and the magnetic pressure of the "guide field" B_y therefore play similar roles in governing equilibrium, described by similar conservation laws.

[13] The conservation of the integral (17) can be identified with the conservation of magnetic helicity [e.g., *Berger and Field*, 1984], $\mathbf{A} \cdot \mathbf{B}$, integrated along the field line, where $\mathbf{A}$ represents a vector potential defining $\mathbf{B} = \nabla \times \mathbf{A}$. This can be seen from a choice of $\mathbf{A}$ given by

$$\mathbf{A} = A\hat{\mathbf{y}} + \mathbf{A}_p \qquad \mathbf{A}_p = -b\nabla A + \nabla F(\alpha, \beta) \tag{20}$$

which gives the same magnetic field (16) as the Euler potentials (15). Here $F(\alpha, \beta)$ is an arbitrary function arising from the freedom of choosing a gauge for the vector potential $\mathbf{A}$ and we use again a gauge in which α and β are conserved in a comoving frame. Then we obtain

$$\mathbf{A} \cdot \mathbf{B} = \alpha B_y \tag{21}$$

Thus the integrated helicity

$$H(\alpha, \beta) = \int \mathbf{A} \cdot \mathbf{B} \frac{ds}{B} = \alpha \int B_y \frac{ds}{B} \tag{22}$$

is proportional to the footpoint displacement Y with a factor α. That means H is also conserved, regardless of the choice of $F(\alpha, \beta)$.

2.4. Conservation Laws Under Topological Changes

[14] So far we have considered the conservation laws in cases without changes in magnetic topology, as satisfied by ideal MHD. However, these conservation laws can be extended to include topological changes, as brought about by reconnection, provided the deviations from ideal MHD are strongly localized, that is, there is no extended slippage or dissipation or heat flux across field lines. This is most easily demonstrated and investigated in simple symmetric configurations. When field lines are broken and reconnected in a configuration with symmetry in x and z, the mass and entropy on the reconnected field lines are the sums of two halves and thus the same as before (see Figure 1 for $S_1(A) = S_2(A)$).

[15] In an asymmetric case, such as at the magnetopause, the reconnecting field lines carry plasmas with different temperature and densities. If we consider again a finite box with symmetry only in the x direction along the magnetic field (see Figure 1), mass and entropy functions on reconnected field lines become the arithmetic means of the functions prior to reconnection, assuming again that slippage and dissipation are highly localized at the reconnection site:

$$M(A) = \frac{1}{2}[M_1(A) + M_2(A)] \tag{23}$$

$$S(A) = \frac{1}{2}[S_1(A) + S_2(A)] \tag{24}$$

Note that S in this case is not a direct function of the total entropy, which is given by the integral (9). In the ideal MHD limit the different entropy densities on the two parts of a reconnected field line do not equilibrate, whereas in the kinetic limit the particle motion along the field would cause such an equilibration, associated with parallel heat flux and

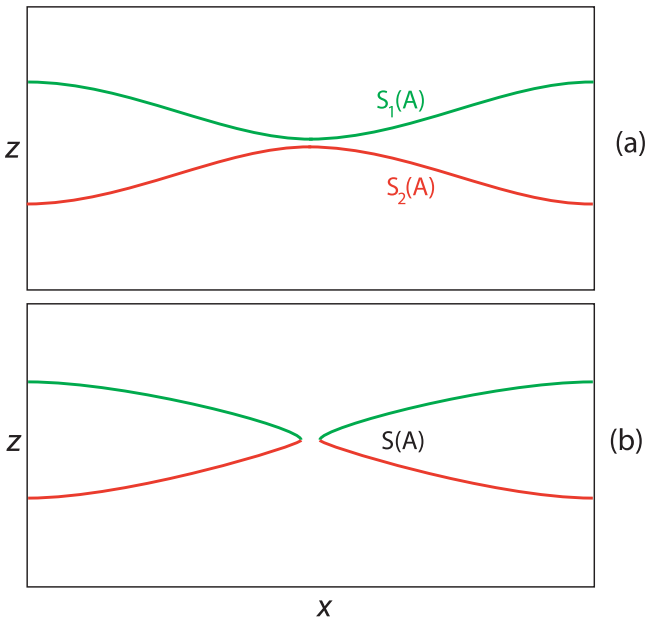

Figure 1. Magnetic field lines (a) just before and (b) just after reconnection. In a fully symmetric case the entropy functions S_1 and S_2 are identical and $S(A) = S_1(A) = S_2(A)$, provided that dissipation is strongly localized. In an asymmetric case, when $S_1(A) \neq S_2(A)$, S is given by $S(A) = [S\ (A) + S_2(A)]/2$ (assuming left-right symmetry).

an entropy increase. If this occurs without energy loss or gain from the flux tube, the final entropy, after equilibration of pressure and temperature then again becomes a function of S given by (24). This has little effect on the magnetic field configuration, which is determined by the balance of pressure and magnetic forces. However, it is important for particle and energy transport along field lines and hence for entry and loss on field lines that have become reconnected at the magnetopause.

[16] In the considerations above we have assumed that M_1, M_2, S_1, and S_2 are nonsingular functions of A, given by the initial configuration. However, considering a standard x-type magnetic field configuration with regular magnetic fields (implying finite field and finite derivatives), it is well known that the flux tube volume (4) diverges logarithmically on field lines approaching an x point. If we assume that the density ρ and the pressure p remain finite in the vicinity of the x point, this would imply that the integrals of mass and pressure per unit magnetic flux also diverge on field lines approaching the x point, contrary to our assumption. How can this apparent contradiction be resolved? Of course, there is a certain vicinity of the x point where the assumption of ideal MHD breaks down. However, if we assume that this vicinity is very small, governed by particle scales, the discrepancy still exists for the region just outside this nonideal region. There are two possibilities to maintain finite mass and entropy integrals. One is that the assumption of regularity of the magnetic field is violated in the limit in which the nonideal region approaches zero. This implies that a derivative of the magnetic field (i.e., the current density) becomes infinite (although remaining integrable). This limit indeed seems approached during an evolution applicable to the substorm growth phase, to be discussed in section 4. The magnetic field structure in that case assumes a cusp structure, which, under different conditions, may also degenerate into two y-type neutral points connected by a singular current sheet [e.g., *Biskamp*, 2003; *Schindler*, 2007, p. 172]. The other alternative is that density and pressure approach zero on field lines connecting to the x point, that is, on the separatrix layers. This alternative, which may be more difficult to realize for large background pressure, seems to be approached during the later phase of the evolution, which in a confined case leads to a new equilibrium (as indicated, for instance, by Figure 3).

3. Comparisons Between MHD and Kinetic Simulations

3.1. Entropy Conservation in the Newton Challenge

[17] The conservation laws discussed in section 2 are based on ideal MHD, generalized, however, to allow for changes in topology. In a fully kinetic model, not only the frozen-in approximation but also entropy conservation may break down through the development of anisotropy and effects of dissipation and heat conduction. *Birn et al.* [2006a] therefore investigated the conservation of the entropy function (7) in a comparison of a particle simulation of magnetic reconnection with an MHD simulation. This study was motivated by a comparative study of forced magnetic reconnection with various particle and fluid codes, named the "Newton challenge" [*Birn et al.*, 2005]. In these simulations, the formation of a thin current sheet and magnetic reconnection were initiated in a plane Harris-type current sheet by temporally limited, spatially varying, inflow of magnetic flux (from top and bottom in Figure 2). All simulations resulted in surprisingly similar final configurations with a concentration of the current in rings around the center of the magnetic islands, as illustrated in Figure 2. This suggested that conservation laws operated similarly in fluid and particle codes despite the fact that kinetic approaches include anisotropy, a different dissipation mechanism, and different waves not included in MHD. This was confirmed by integrating mass M and entropy function S along field lines, as functions of the flux variable A obtained from integrating the magnetic field along the boundary of the simulation box.

[18] Figures 3a and 3b show mass M and entropy S obtained in this way from (5) and (7), respectively, as functions of A, for both MHD (red solid lines) and PIC simulations (green dashed lines) at late stages of the simulations, together with the initial distribution (dotted lines). Figure 3c shows the corresponding pressure variations, also averaged over the field lines. For the PIC simulation the pressure p was defined by the trace of the full pressure tensor, given by (13); however, using (14) instead made no visible difference.

[19] The mass and entropy functions in Figure 3 show remarkable agreement with each other and with the initial distribution, despite the fact that most field lines at the late times have undergone reconnection. This demonstrates the absence of slippage and that dissipation leads only to a minimal increase in the total entropy on a field line. In contrast, the pressure functions $P(A)$ have changed drastically from the initial distribution but agree closely between

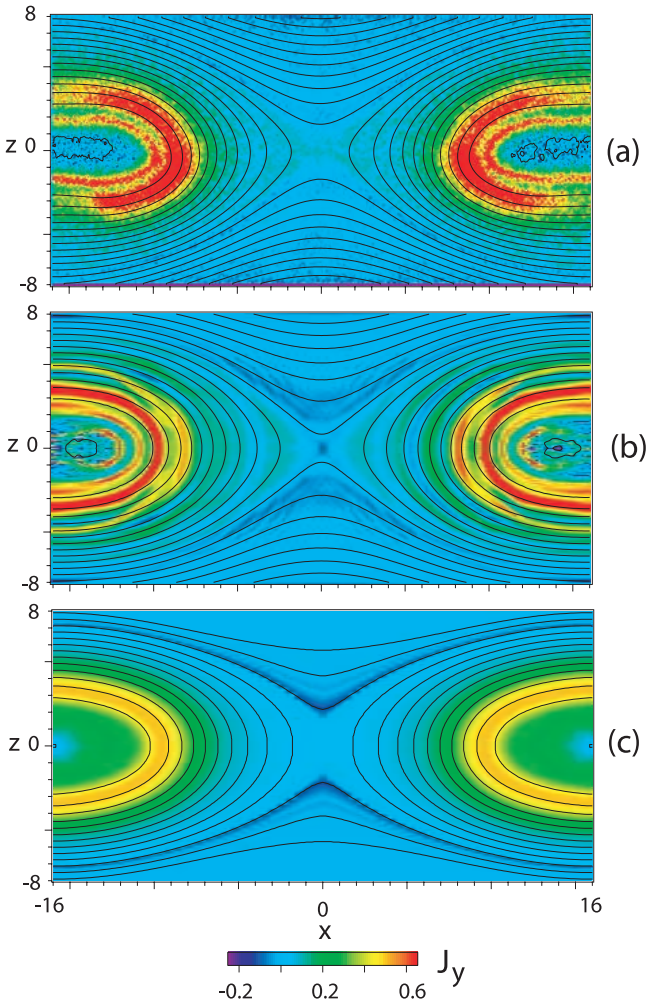

Figure 2. Late magnetic field configurations and current density (color) for simulations of the Newton challenge problem [*Birn et al.*, 2005, 2006a]: (a) PIC simulation, (b) MHD simulation, and (c) a minimum energy equilibrium for the same entropy function $S(A)$ as for the initial Harris sheet and a boundary deformation roughly consistent with the simulations [*Zaharia and Birn*, 2007].

MHD and PIC simulations. The small difference is largely due to the fact that the PIC simulation has evolved slightly more than the MHD simulation. This can be inferred from the small local peaks visible in $M(A)$ and $S(A)$. These peaks are associated with a divergence of the flux tube volume $V(A)$ on field lines that connect to the x point (assuming that the magnetic field is regular) and thus indicate the flux value at the x point. In the PIC simulation this location has proceeded to slightly larger values of $|A|$.

[20] Figure 4 demonstrates that the (approximate) conservation of the entropy function $S(A)$ applies not only to the quasi-equilibrium states approached in the late phase of the simulation but even during the rapid changes near the time of fastest reconnection. Close inspection of Figure 4 reveals a slight increase of $S(A)$ after reconnection, that is, for A values to the right of the little peaks of $S(A)$. This is the effect of the dissipation, which is necessary to enable reconnection, but nevertheless has only minor effect on the heating.

3.2. Newton Challenge With Guide Field

[21] As mentioned in section 2, in 2.5-D cases with invariance in the y direction there is another conserved quantity, the displacement of boundary footpoints $Y(A)$ of field lines in the y direction, illustrated by Figure 5. However, it is not obvious that this quantity should be conserved through reconnection, as suggested by Figure 5. Figure 6a shows results from simulations of the Newton challenge problem including an (initially) constant guide

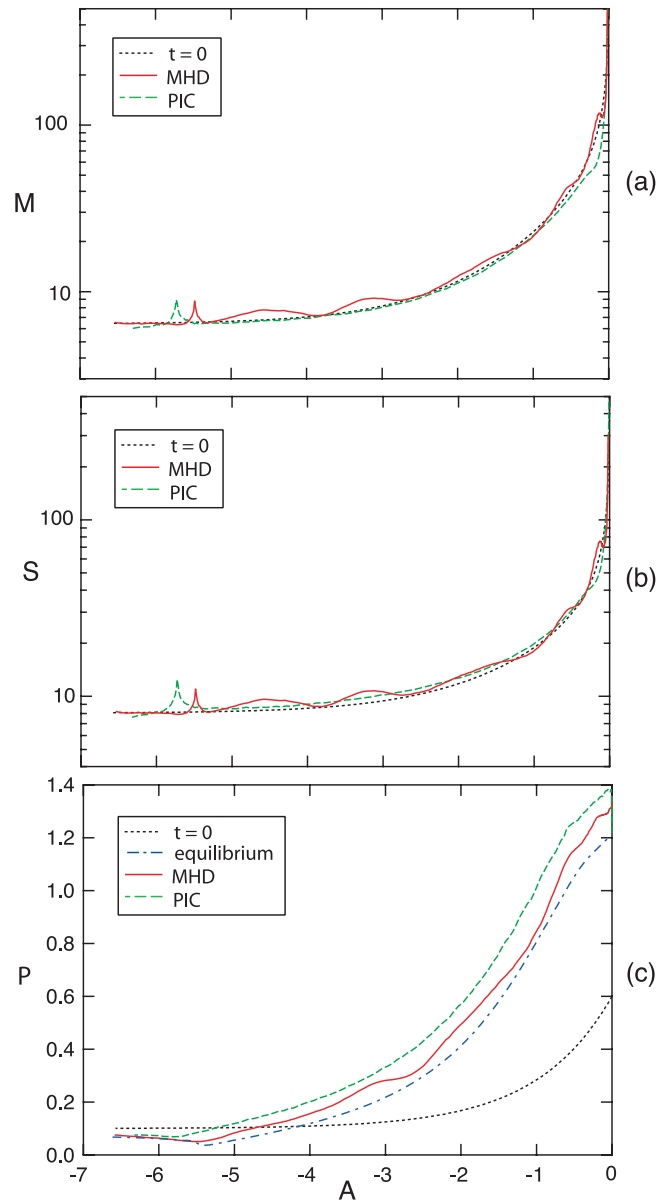

Figure 3. (a) Mass M, (b) entropy S, and (c) pressure p as functions of the magnetic flux variable A for MHD (red lines) and PIC simulations (green dashed lines) of the Newton challenge problem [*Birn et al.*, 2005] in comparison to the initial functions (black dotted lines). Also shown is the pressure function of a minimum energy equilibrium state based on the initial entropy function (blue dash-dotted line). Modified after *Birn et al.* [2006a] and *Zaharia and Birn* [2007].

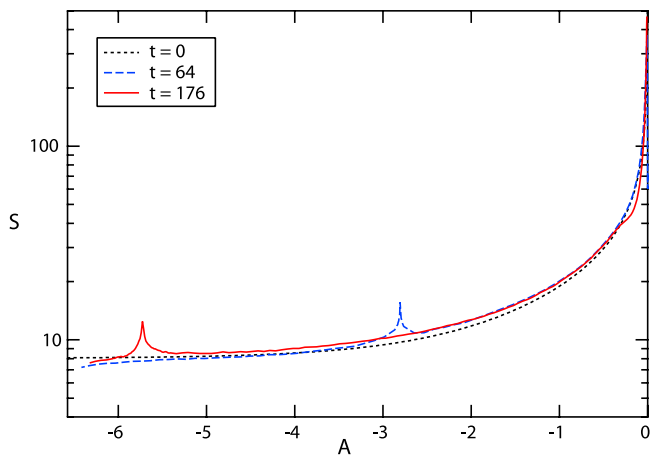

Figure 4. Entropy function S for a PIC simulation of the Newton challenge problem [*Birn et al.*, 2005] for three different times; t = 64 corresponds to the time of fastest reconnection.

field with a magnitude of 0.8 (in units of the antiparallel field component), demonstrating that this is indeed the case for both MHD and PIC simulations. We note that $Y(A)$ should diverge at the separatrix when the B field remains regular. This is evidenced by the local peaks in Y in Figure 6a, which proceed to smaller values of A as reconnection advances. The guide field functions $B(A)$ (Figure 6b) change considerably from the initially constant value 0.8. The basic changes are similar for MHD and PIC; however, the final functions differ somewhat, probably due to the fact that the PIC simulation has proceeded farther, i.e., reconnected more flux, as indicated by the A values at the separatrices.

3.3. Adiabatic Equilibrium States

[22] Figures 2 and 3 also contain results from an equilibrium calculation using the entropy function $S(A)$ of the initial Harris sheet and a boundary deformation consistent with those in the simulations [*Zaharia and Birn*, 2007]. An iteration scheme was used to arrive at a final minimum energy state with the topology as resulting from reconnection. Figure 2c shows the same characteristics as the

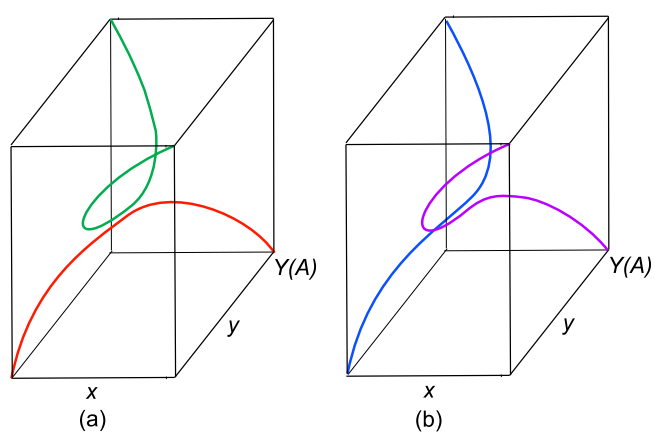

Figure 5. Schematic of magnetic field lines (a) just before and (b) just after reconnection in the presence of a guide field B_y.

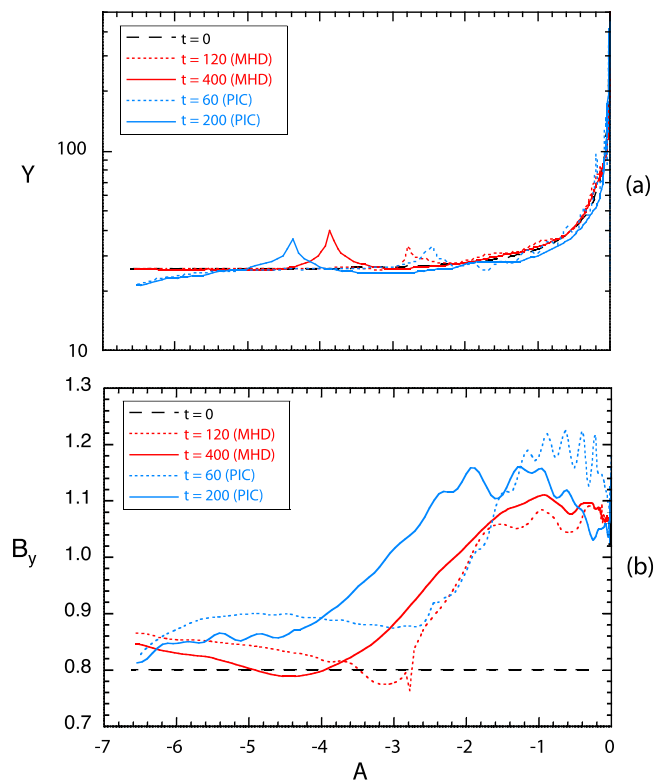

Figure 6. (a) Footpoint displacement Y and (b) guide field B_y as functions of the magnetic flux variable A for MHD (red lines) and PIC simulations (blue lines) of a Newton challenge problem with initially uniform guide field, in comparison to the initial functions (dotted lines).

simulations, although the current density in the rings appears slightly lower, consistent with a smoothed result of the simulations. The pressure function $p(A)$ in Figure 3c also shows a very good agreement with the late simulation results.

[23] The approximate conservation of the entropy function $S(A)$, given by (7), and of the displacement $Y(A)$ has important consequences for the amount of energy that can be released by reconnection, which is often estimated by comparing an initial stressed state with a current-free, i.e., potential field configuration satisfying the same boundary conditions as the initial state. This is demonstrated by Figure 7, which shows the magnetic energy release from reconnection of an initial Harris sheet for various values of the polytropic index γ. Square symbols show the magnetic energy of minimum energy states, obtained from the adiabatic equilibrium approach for entropy conservation [*Zaharia and Birn*, 2007], while cross symbols represent late MHD simulation results. The results were obtained for a box that was twice as wide in z as the box of the Newton challenge simulations but without boundary perturbations. The amount of energy released clearly depends on the value of γ, that is, on the thermodynamic model. Incompressible models ($\gamma \rightarrow \infty$) release the smallest amount of energy, while isothermal models ($\gamma = 1$) release significantly more, due to the (implied) assumption of infinite thermal conductivity. For comparison, the magnetic energy of a potential field with the same boundary conditions is $W_{pot} \approx 12$. Thus

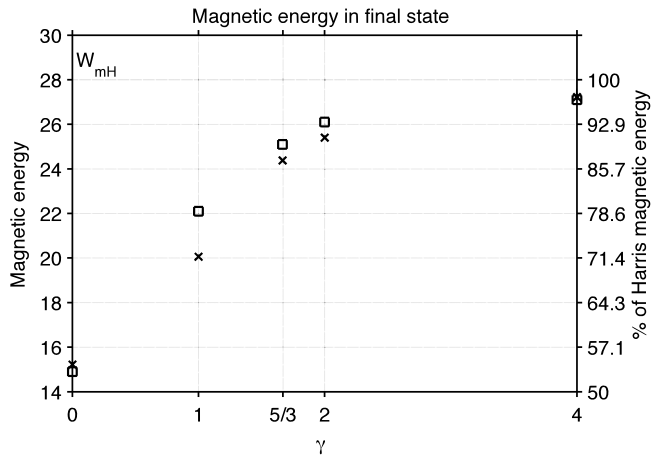

Figure 7. Magnetic energy release from reconnection of an initial Harris sheet for various values of the polytropic index γ, showing the magnetic energy of the final reconnected state, obtained for entropy conservation (square symbols), in comparison to late MHD simulation results (cross symbols). After *Zaharia and Birn* [2007].

the energy release under more realistic adiabatic constraints is significantly lower than an estimate based on the excess energy over a potential field or the field governed by the same pressure function $p(A)$ as the Harris sheet. Releasing this additional amount of energy requires conduction across field lines, losses through the boundaries, collisions, and/or radiative losses. All of these are small in magnetospheric reconnection but may play a more significant role for solar flare energy releases, albeit on a time scale that is much larger than that of the initial, impulsive phase.

4. Substorm Growth Phase: Thin Current Sheet Formation, Loss of Equilibrium

[24] Entropy conservation apparently plays a crucial role in governing the substorm growth phase and the evolution of the magnetotail toward instability or loss of equilibrium. *Erickson and Wolf* [1980] and *Schindler and Birn* [1982] investigated the possibility of steady, adiabatic, i.e., entropy conserving, convection in the magnetotail and concluded that earthward transport of magnetic flux tubes would lead to an unrealistically large pressure buildup in the near tail. They suggested that sunward convection in the tail therefore should be time-dependent, leading into a sudden, nonadiabatic release associated with substorms.

[25] More recently, *Birn and Schindler* [2002] investigated the quasi-static response of the magnetotail to a deformation of the magnetopause boundary. Using two-dimensional magnetohydrostatic equilibrium theory, together with flux, entropy, and topology conservation (equivalent to ideal MHD for slow, quasi-static, evolution), they demonstrated that a finite boundary deformation of magnetotail equilibria can lead to a critical state at which neighboring equilibria that satisfy the constraints cease to exist. The critical state is characterized by a strong local current density enhancement, that is, the formation of a thin current sheet. These results were confirmed by (ideal) MHD simulations, including also three-dimensional configurations [*Birn et al.*, 2004a] and tailward propagating boundary deformations [*Birn et al.*, 2003].

[26] Figure 8 illustrates the major result. Figure 8a shows a configuration near the critical state, characterized by a thin sheet with strongly enhanced current density (color) embedded in the plasma sheet. This sheet bifurcates into two sheets toward the Earth (to the left in Figure 8). Figure 8b shows the maximum current density in the tail as a function of the amplitude a of the boundary indentation, which diverges at a finite value of a. The two curves correspond to two different scales of the deformation along the x direction, given by the parameter Δp, where larger Δp corresponds to a larger scale in x. This demonstrates that the critical limit depends not only on the amplitude of the boundary perturbation but also on the scale length.

[27] The strong current density enhancement associated with the critical state obviously renders the tail unstable to current-driven instabilities and magnetic reconnection. These results thus provide a very strong argument that slow adiabatic deformations of the magnetotail resulting from the solar wind interaction can drive the magnetotail into a "catastrophe" or the onset of instability, regardless of how dissipation sets in near the critical state. These results also demonstrate the close relationship between external perturbations imposed by the solar wind and the formation of a thin current sheet, although the direct association with an external trigger, such as the northward turning of the interplanetary magnetic field [e.g., *McPherron et al.*, 1986; *Lyons*, 1996], could not be verified yet.

[28] The results discussed so far are based on ideal MHD theory and simulations, with entropy conservation (3), or in

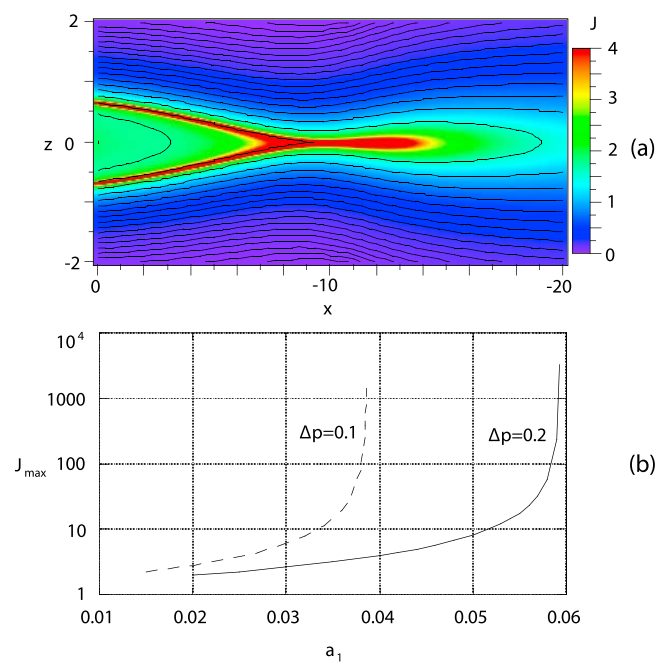

Figure 8. Response of the magnetotail to adiabatic deformation [*Birn and Schindler*, 2002]: (a) magnetotail configuration near the critical limit, consisting of a thin embedded current sheet (color scale) that bifurcates toward the Earth (to the left) and (b) maximum current density as function of the amplitude a of the boundary indentation for two scaling parameters Δp.

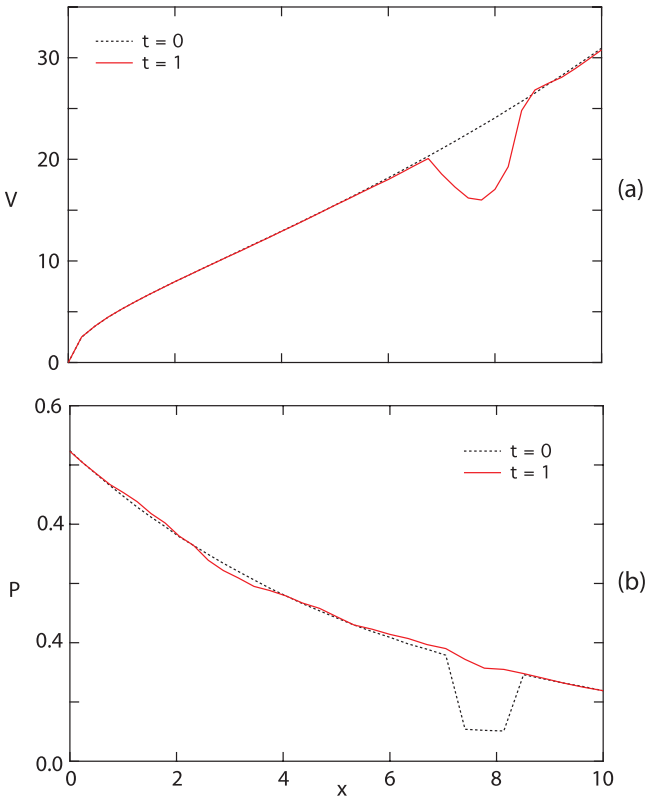

Figure 9. Variation of (a) flux tube volume V and (b) pressure along the x axis after relaxation of an initial pressure depletion of a localized flux tube. The dotted lines show the initial variation; the solid lines show the variation after one Alfvén time. Based on the simulations of *Birn et al.* [2004b].

integral form (7), imposed. However, when the current sheet thickness approaches typical ion scales, the MHD approximations break down and a more rigorous kinetic approach becomes necessary. Such an approach, using the Vlasov formalism, has been outlined by *Schindler* [2007, section 8.5], for two-dimensional equilibria, replacing the invariance of the entropy function with the invariance of phase space volume. For the limit of small gyroradii *Schindler* [2007] demonstrated the equivalence of this approach with the fluid approach. Models based on gyro-averaged motion, including pitch angle scattering to maintain pressure isotropy, gave similar results to ideal MHD [*Wolf*, 1983; *Garner et al.*, 2003]. Although a full generalization to collisionless plasmas is not available, the comparisons between MHD and PIC simulations, discussed in section 3, further support the view that the ideal MHD adiabatic constraint (7) remains a good approximation even when the current sheet thickness approaches ion scales.

[29] Another question is whether, during the adiabatic deformation, the tail remains stable to ideal MHD instabilities until the critical threshold is reached. The most relevant ideal MHD instability is the ballooning mode, driven by "unfavorable" pressure gradients in the direction of the curvature vector of field lines, which is satisfied for typical magnetotail equilibria. However, compressibility provides a stabilizing term so that the stability properties are not obvious. Both stable [e.g., *Lee and Wolf*, 1992; *Lee*, 1999] and unstable cases [e.g., *Bhattacharjee et al.*, 1998; *Miura*, 2001; *Cheng and Zaharia*, 2004] have been found. The analysis by *Schindler and Birn* [2004] indicated that, at least in the ideal MHD limit for 2D equilibria, differences in stability can be attributed to differences in the underlying equilibrium. The criterion for ballooning instability can be linked to a general interchange stability criterion that involves the variation of flux tube entropy S [e.g., *Bernstein et al.*, 1958; *Schindler and Birn*, 2004]. The conclusion is that typical tail equilibria, for which the pressure decreases monotonically down the tail, are stable when the entropy measure $S = p^{1/\gamma}V$ increases monotonically. The conservation of the entropy function $S(A)$ then insures that a configuration that is initially stable, corresponding to a monotonic increase in S, remains stable as long as the topology does not change, that is, until the critical state is reached or nonideal instability sets in, driven by the current intensification.

5. Entropy Loss From Plasmoid Ejection, Propagation of Bubbles

[30] The results discussed in section 4 demonstrate the important role of entropy conservation in governing the substorm growth phase and leading to onset of instability or loss of equilibrium. The strong current density enhancement associated with this process can be expected to initiate reconnection, regardless of the details of the dissipation mechanism, causing the pinching off of field lines and the ejection of a plasmoid. The severance of parts of closed field lines reduces the entropy content of the shortened parts. This has two important consequences: (1) the entropy depletion is an important factor in permitting the penetration of depleted magnetic flux tubes ("bubbles") closer to the Earth [*Pontius and Wolf*, 1990; *Chen and Wolf*, 1993, 1999; *Birn et al.*, 2004b] and (2) the entropy loss changes the entropy function $S(A)$ and generates a localized decrease which enables the unstable growth of ballooning modes and provides smaller-scale cross-tail structure to the earthward collapsing field lines [*Birn et al.*, 2006b].

[31] Using three-dimensional MHD simulations, *Birn et al.* [2004b] investigated the propagation of low-entropy bubbles in the magnetotail, generated by a localized reduction of pressure. This mechanism apparently differs from the severance process, which is expected to reduce the volume of a flux tube without (initially) changing the pressure. However, using the simulations of *Birn et al.* [2004b], we found that after a rapid adjustment to the initial force imbalance, the reduced-entropy flux tubes assume a reduced volume while the pressure increases to reestablish approximate force balance. This is demonstrated by Figure 9, which shows the initial variation of the flux tube volume V and pressure p along the x axis (dotted lines) together with the variations after one Alfvén time (solid lines), equivalent to a few seconds.

[32] *Birn et al.* [2004b] also confirmed that the depletion is crucial in permitting the earthward propagation of a bubble. Figure 10a illustrates this result by a comparison of three simulations, one starting with a depleted flux tube (solid line), one with additional added initial earthward momentum (dashed line), and one with initial momentum

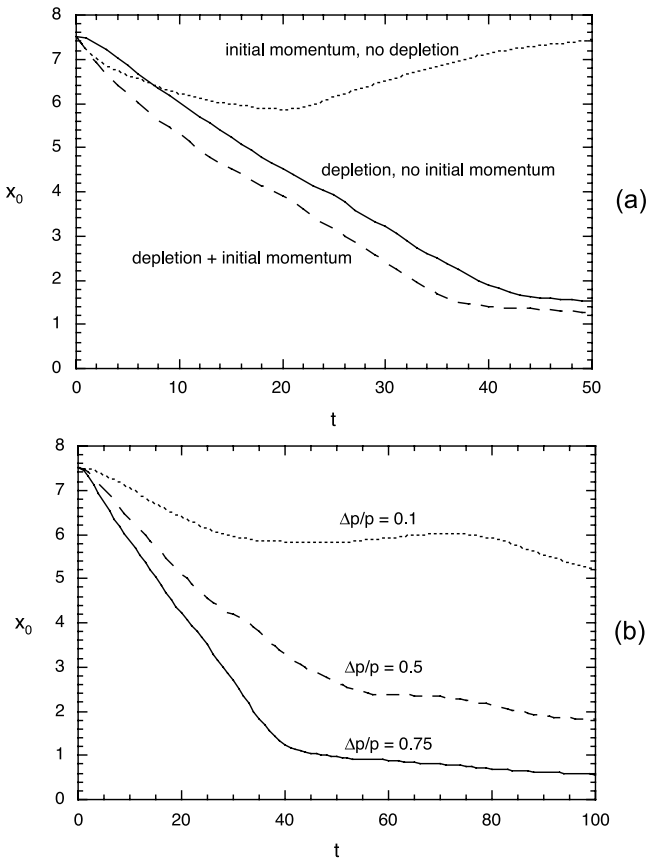

Figure 10. Earthward penetration of entropy-depleted flux tubes (bubbles), showing the equatorial intersection x_0 as function of time (a) for pressure reduction but no initial velocity (solid line), pressure reduction and initial velocity (dashed line), no pressure reduction but finite initial velocity (dotted line), and (b) for various amplitudes of initial pressure (and entropy) reduction. Based on the simulations of *Birn et al.* [2004b].

but without depletion (dotted line). Obviously, simple acceleration without depletion does not lead to significant earthward propagation, whereas the two depleted flux tubes, after some initial phase, show similar evolution and propagation toward Earth. This result can be considered as the consequence of interchange instability, originally postulated by *Pontius and Wolf* [1990]. Figure 10b demonstrates that the penetration to Earth depends on the entropy reduction, here imposed by a pressure reduction. More strongly depleted flux tubes obviously penetrate closer.

[33] The dependence of the depth of penetration on the amount of depletion may also affect the average mass and entropy variation. Since field lines with lower mass and entropy content may penetrate closer to Earth than those with higher content, the observed average decrease of mass and entropy content toward the Earth [*Borovsky et al.*, 1998; *Kaufmann et al.*, 2004] even earthward of the typical near-Earth reconnection site at $\sim 20R_E$ distance downtail may be the consequence of such spatial variation of deposition, rather than result from a nonadiabatic energy loss mechanism or from precipitation into the ionosphere. Such a spatial variation in deposition may even result from a single event. Let us consider the progress of reconnection in the near tail from the central plasma sheet to lobe field lines. When the location of reconnection stays roughly the same in the near tail, the major temporal change of the entropy function S for newly reconnected field lines stems from the decrease of pressure while the flux tube volume changes very little. Therefore field lines that are reconnected later have lower mass and entropy content and can therefore penetrate closer to Earth than those reconnected earlier.

[34] In the discussion above we have focused on the behavior of single flux tubes. However, the change of the stability properties of the tail to ballooning or interchange modes, resulting from the plasmoid loss, may also contribute to the structuring of the depleted region in the cross-tail direction [e.g., *Sergeev et al.*, 1996]. This effect was demonstrated by *Birn et al.* [2006b]. It is illustrated by Figure 11, which shows the earthward flow speed (color scale) and the depleted region associated with a propagating bubble at three different times in the x,y plane. These plots demonstrate that the bubble, which originally consists of a single connected flux tube, breaks apart into several pieces of flux tubes. This is presumably the result of ballooning modes with a wave structure in the cross-tail direction.

6. Summary and Discussion

[35] We have discussed how entropy conservation and the loss of entropy might affect the evolution of the magnetotail, particularly in relation to substorms, including the growth phase, onset, and substorm expansion. Results from quasi-static theory and MHD simulations demonstrated how entropy conservation, together with flux and topology conservation, may govern the growth phase evolution toward a loss of equilibrium in response to perturbations imposed by the solar wind. The critical state at which this takes place is characterized by the formation of a very thin intense current sheet embedded within the thicker plasma/current sheet. This strong current density intensification suggests the onset of instability or a catastrophe, that is, loss of equilibrium, regardless of the dissipation mechanism, which then leads to the onset of reconnection and plasmoid formation and ejection.

[36] The subsequent loss of entropy by the severance of a plasmoid may affect the dynamic evolution in two ways. As suggested by *Pontius and Wolf* [1990] and confirmed by 3D MHD simulations [*Birn et al.*, 2004b], the loss of entropy is essential in enabling depleted closed flux tubes (bubbles) to penetrate to the inner magnetosphere closer to Earth. Here we further demonstrated that the penetration depth, and thus the location where depleted flux tubes are deposited, depends on the amount of depletion. This might explain a statistical decrease of the mass and entropy content of magnetic flux tubes from the tail reconnection site toward the Earth [*Borovsky et al.*, 1998], even without the need for losses to the ionosphere. In addition, the entropy reduction may change the stability properties of the tail, enabling interchange or ballooning instabilities. Such instabilities may then be responsible for providing cross-tail structure and filamentation of bubbles or localized fast flow bursts in the tail [e.g., *Goertz and Baumjohann*, 1991; *Sergeev et al.*, 1996].

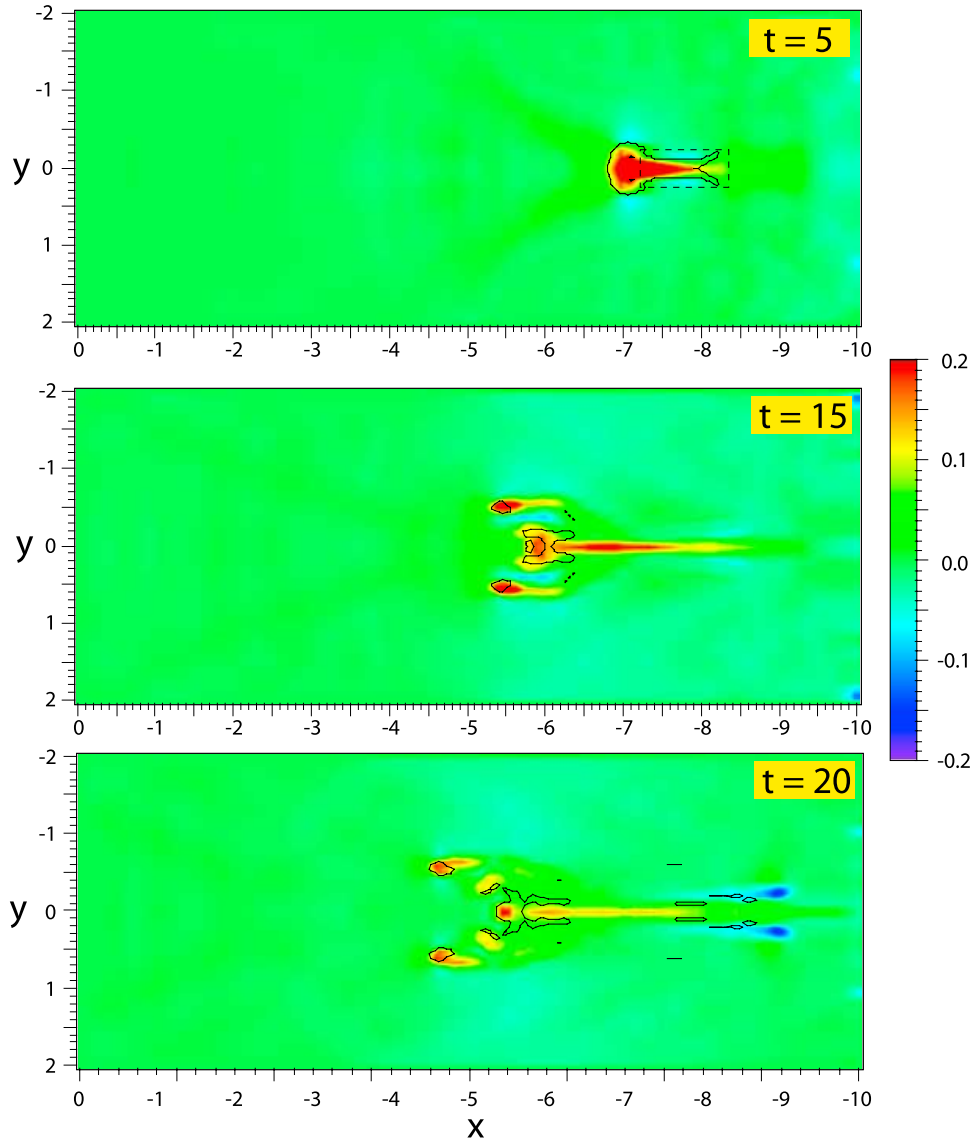

Figure 11. Evolution of an entropy-depleted flux tube (bubble), showing properties in the equatorial plane. The color scale shows the earthward flow speed, and the contours show the boundary of the region of reduced entropy density. The dashed rectangle in Figure 11 (top) indicates the initially depleted region.

[37] These results are based on conservation of an entropy integral (7) applied to magnetic flux tubes, which is imposed in the MHD model. However, as demonstrated by the comparison between MHD and full particle simulations, the integral entropy measure is well conserved on moving flux tubes in particle simulations as well, even during rapid evolution, providing credence to the results of the MHD simulations. The (approximate) conservation of this entropy function, even through the reconnection process, is a consequence of the strong localization of Joule dissipation (given by $\mathbf{j} \cdot \mathbf{E}'$, where $\mathbf{E}' = \mathbf{E} + \mathbf{v} \times \mathbf{B}$) and of the lack of significant slippage and heat flux across the magnetic field. We note here that the agreement between the entropy conservation in fluid and particle simulations was obtained for two-dimensional configurations and does not necessarily remain valid in three dimensions. Also the agreement was shown for an evolution on relatively short, Alfvénic, time scales. For variations on longer time scales, the single-fluid entropy conservation might become violated, for instance, as a result of energy-dependent particle drifts across the magnetic field.

[38] **Acknowledgments.** This work was performed under the auspices of the U.S. Department of Energy, supported by a grant from NASA Goddard Space Flight Center and by NASA's Heliophysics Theory Program.

[39] Wolfgang Baumjohann thanks the reviewers for their assistance in evaluating this paper.

References

Berger, M. A., and G. B. Field (1984), The topological properties of magnetic helicity, *J. Fluid Mech.*, *147*, 133.

Bernstein, I. B., E. A. Frieman, M. D. Kruskal, and R. M. Kulsrud (1958), An energy principle for hydromagnetic stability problems, *Proc. R. Soc. London, Ser. A*, *244*, 17.

Bhattacharjee, A., Z. W. Ma, and X. Wang (1998), Ballooning instability of a thin current sheet in the high-Lundquist-number magnetotail, *Geophys. Rev. Lett.*, *25*, 861.

Birn, J., and K. Schindler (2002), Thin current sheets in the magnetotail and the loss of equilibrium, *J. Geophys. Res.*, *107*(A7), 1117, doi:10.1029/2001JA000291.

Birn, J., K. Schindler, and M. Hesse (2003), Formation of thin current sheets in the magnetotail: Effects of propagating boundary deformations, *J. Geophys. Res.*, *108*(A9), 1337, doi:10.1029/2002JA009641.

Birn, J., J. C. Dorelli, M. Hesse, and K. Schindler (2004a), Thin current sheets and loss of equilibrium: Three-dimensional theory and simulations, *J. Geophys. Res.*, *109*, A02215, doi:10.1029/2003JA010275.

Birn, J., M. Hesse, and K. Schindler (2004b), On the propagation of bubbles in the geomagnetic tail, *Ann. Geophys.*, *22*, 1773.

Birn, J., et al. (2005), Forced magnetic reconnection, *Geophys. Res. Lett.*, *32*, L06105, doi:10.1029/2004GL022058.

Birn, J., M. Hesse, and K. Schindler (2006a), Entropy conservation in simulations of magnetic reconnection, *Phys. Plasmas*, *13*, 092117.

Birn, J., M. Hesse, and K. Schindler (2006b), On the role of entropy conservation and entropy loss governing substorm phases, in *Proceedings of the Eighth International Conference of Substorms*, edited by M. Syrjäsuo and E. Donovan, p. 19, Univ. of Calgary, Calagary, Canada.

Biskamp, D. (2003), *Nonlinear Magnetohydrodynamics*, Cambridge Univ, Press, Cambridge, U. K.

Borovsky, J. E., M. F. Thomsen, R. C. Elphic, T. E. Cayton, and D. J. McComas (1998), The transport of plasma sheet material from the distant tail to geosynchronous orbit, *J. Geophys. Res.*, *103*, 20,297.

Chen, C. X., and R. A. Wolf (1993), Interpretation of high-speed flows in the plasma sheet, *J. Geophys. Res.*, *98*, 21,409.

Chen, C. X., and R. A. Wolf (1999), Theory of thin-filament motion in Earth's magnetotail and its application to bursty bulk flows, *J. Geophys. Res.*, *104*, 14,613.

Cheng, C. Z., and S. Zaharia (2004), MHD ballooning instability in the plasma sheet, *Geophys. Res. Lett.*, *31*, L06809, doi:10.1029/2003GL018823.

Chew, G. F., M. L. Goldberger, and F. E. Low (1956), The Boltzmann equation and the one-fluid hydromagnetic equations in the absence of particle collisions, *Proc. R. Soc. London, Ser. A*, *236*, 112.

Erickson, G. M., and R. A. Wolf (1980), Is steady convection possible in the Earth's magnetotail?, *Geophys. Res. Lett.*, *7*, 897.

Garner, T. W., R. A. Wolf, R. W. Spiro, M. F. Thomsen, and H. Korth (2003), Pressure balance inconsistency exhibited in a statistical model of magnetospheric plasma, *J. Geophys. Res.*, *108*(A8), 1331, doi:10.1029/2003JA009877.

Goertz, C. K., and W. Baumjohann (1991), On the thermodynamics of the plasma sheet, *J. Geophys. Res.*, *96*, 20,991.

Hesse, M., and D. Winske (1998), Electron dissipation in collisionless magnetic reconnection, *J. Geophys. Res.*, *103*, 26,479.

Kaufmann, R. L., W. R. Paterson, and L. A. Frank (2004), Pressure, volume, density relationships in the plasma sheet, *J. Geophys. Res.*, *109*, A08204, doi:10.1029/2003JA010317.

Lee, D. (1999), Stability analysis of the plasma sheet using hall magnetohydrodynamics, *J. Geophys. Res.*, *104*, 19,993.

Lee, D., and R. Wolf (1992), Is the Earth's magnetotail balloon unstable?, *J. Geophys. Res.*, *97*, 19,251.

Lyons, L. R. (1996), Substorms: Fundamental observational features, distinction from other disturbances, and external triggering, *J. Geophys. Res.*, *101*, 13,011.

Lyons, L. R., and D. C. Pridmore-Brown (1990), Force balance near an X-line in a collisionless plasma, *J. Geophys. Res.*, *95*, 20,903.

McPherron, R. L., T. Terasawa, and A. Nishida (1986), Solar wind triggering of substorm onsets, *J. Geomagn. Geoeletr.*, *38*, 1089.

Miura, A. (2001), Ballooning instability as a mechanism of the near-Earth onset of substorms, *Space Sci. Rev.*, *95*, 1387.

Pontius, D., and R. A. Wolf (1990), Transient flux tubes in the terrestrial magnetosphere, *Geophys. Res. Lett.*, *17*, 49.

Pritchett, P. L. (1994), Effect of electron dynamics on collisionless reconnection in two-dimensional magnetotail equilibria, *J. Geophys. Res.*, *99*, 5935.

Schindler, K. (2007), *Physics of Space Plasma Activity*, Cambridge Univ. Press, Cambridge, U. K.

Schindler, K., and J. Birn (1982), Self-consistent theory of time-dependent convection in the Earth's magnetotail, *J. Geophys. Res.*, *87*, 2263.

Schindler, K., and J. Birn (2004), MHD stability of magnetotail equilibria including a background pressure, *J. Geophys. Res.*, *109*, A10208, doi:10.1029/2004JA010537.

Sergeev, V. A., V. Angelopoulos, J. T. Gosling, C. A. Cattell, and C. T. Russell (1996), Detection of localized, plasma-depleted flux tubes or bubbles in the midtail plasma sheet, *J. Geophys. Res.*, *101*, 10,817.

Shay, M. A., and J. F. Drake (1998), The role of electron dissipation on the rate of collisionless magnetic reconnection, *Geophys. Res. Lett.*, *25*, 3759.

Vasyliūnas, V. M. (1975), Theoretical models of magnetic field line merging, 1, *Rev. Geophys. Space Phys.*, *13*, 303–336.

Wolf, R. A. (1983), The quasi-static (slow-flow) region of the magnetosphere, in *Solar-Terrestrial Physics: Principles and Theoretical Foundations*, edited by R. L. Carovillano and J. M. Forbes, pp. 303–368, D. Reidel, Dordrecht, Netherlands.

Wolf, R. A., V. Kumar, F. R. Toffoletto, G. M. Erickson, A. M. Savoie, C. X. Chen, and C. L. Lemon (2006), Estimating local plasma sheet $PV^{5/3}$ from single-spacecraft measurements, *J. Geophys. Res.*, *111*, A12218, doi:10.1029/2006JA012010.

Zaharia, S., and J. Birn (2007), Adiabatic plasma equilibria and application to a reconnection problem, *Phys. Plasmas*, *14*, 07210.

J. Birn and S. Zaharia, Space Science and Applications Group, Los Alamos National Laboratory, Los Alamos, NM 87545, USA. (jbirn@lanl.gov)

M. Hesse, NASA Goddard Space Flight Center, Greenbelt, MD 20771, USA.

K. Schindler, Institut für Theoretische Physik, Ruhr-Universität Bochum, D-44780 Bochum, Germany.